

Spin resonance free electron ring injector

V. Ranjbar

January 2017

Collider Accelerator Department
Brookhaven National Laboratory

U.S. Department of Energy

USDOE Office of Science (SC), Nuclear Physics (NP) (SC-26)

Notice: This technical note has been authored by employees of Brookhaven Science Associates, LLC under Contract No. DE-SC0012704 with the U.S. Department of Energy. The publisher by accepting the technical note for publication acknowledges that the United States Government retains a non-exclusive, paid-up, irrevocable, world-wide license to publish or reproduce the published form of this technical note, or allow others to do so, for United States Government purposes.

DISCLAIMER

This report was prepared as an account of work sponsored by an agency of the United States Government. Neither the United States Government nor any agency thereof, nor any of their employees, nor any of their contractors, subcontractors, or their employees, makes any warranty, express or implied, or assumes any legal liability or responsibility for the accuracy, completeness, or any third party's use or the results of such use of any information, apparatus, product, or process disclosed, or represents that its use would not infringe privately owned rights. Reference herein to any specific commercial product, process, or service by trade name, trademark, manufacturer, or otherwise, does not necessarily constitute or imply its endorsement, recommendation, or favoring by the United States Government or any agency thereof or its contractors or subcontractors. The views and opinions of authors expressed herein do not necessarily state or reflect those of the United States Government or any agency thereof.

Spin Resonance Free Electron Ring Injector

V.H. Ranjbar, M. Blaskiewicz, F. Meot, C. Montag, S. Tepikian,
Brookhaven National Lab, Upton NY 11973
 (Dated: January 3, 2017)

We have developed an intrinsic resonance free circular electron accelerator. This lattice could be placed in the existing RHIC tunnel and accelerate electrons from 100 MeV to 20 GeV avoiding all major polarization loss usual in such machines.

I. INTRODUCTION

We present a spin resonance free electron ring injector for an electron ion collider. Such an accelerator will provide spin polarized electrons for energies up to 20 GeV. The proposed device will fit in the existing RHIC tunnel, employ standard technology, and accelerate an electron bunch to top energy in about 5-50 msecs. In the past it was believed that such a device would cause profound polarization loss due the combined effects of many depolarizing resonances. However we have recently devised a lattice which by virtue of the symmetry of construction and high operating tunes, avoids all significant depolarization sources in the energy range of its operation.

II. SPIN RESONANCE REVIEW

The dynamics of the spin vector of a charged particle with q charge in the laboratory frame is described by the Thomas-BMT equation,

$$\frac{d\vec{S}}{dt} = \frac{q}{\gamma m} \vec{S} \times \left((1 + G\gamma)\vec{B}_\perp + (1 + G)\vec{B}_\parallel \right), \quad (1)$$

\vec{S} is the spin vector of a particle in the rest frame, and \vec{B}_\perp and \vec{B}_\parallel are defined in the laboratory rest frame with respect to the particle's velocity. $G = \frac{g-2}{2}$ is the anomalous magnetic moment coefficient, and γmc^2 is the energy of the particle. Here we neglect the electric fields. This equation is usually transformed by expanding about a reference orbit described by the Frenet-Serret coordinate system shown in Fig. 1. Thus we have

$$\frac{d\hat{x}}{ds} = \frac{\hat{s}}{\rho}, \quad \frac{d\hat{s}}{ds} = -\frac{\hat{x}}{\rho}, \quad \text{and} \quad \frac{d\hat{z}}{ds} = 0, \quad (2)$$

where ρ is the local radius of curvature for the reference orbit. This is satisfactory for a trajectory in the plane (no vertical bends). Particle motion can be parameterized in this coordinate system as,

$$\vec{r} = \vec{r}_o(s) + x\hat{x} + z\hat{z}. \quad (3)$$

Here, $\vec{r}_o(s)$ is the reference orbit, and $\hat{s} = d\vec{r}_o/ds$. Also since we are concerned only with spin 1/2 particles, we can employ the well-developed spinor formalism. Together, following a standard derivation¹, this yields a new form of the Thomas-BMT equation:

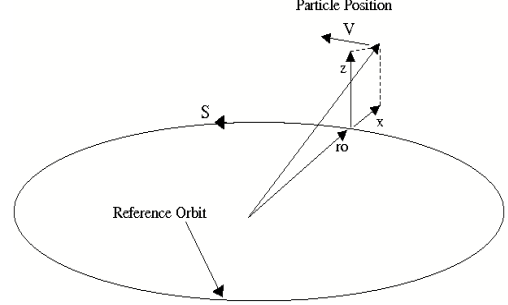


FIG. 1. The curvilinear coordinate system for a particle motion in a circular accelerator. \hat{x} , \hat{s} and \hat{z} are the transverse radial, the longitudinal, and the transverse vertical unit basis vectors, and $\vec{r}_o(s)$ is the reference orbit.

$$\frac{d\Psi}{d\theta} = -\frac{i}{2} \begin{pmatrix} f_3 & -\xi \\ -\xi^* & -f_3 \end{pmatrix} \Psi. \quad (4)$$

Where $\xi(\theta) = F_1 - iF_2$ and $f_3 = (1 + F_3)$ with,

$$\begin{aligned} F_1 &= -\rho z''(1 + G\gamma) \\ F_2 &= (1 + G\gamma)z' - \rho(1 + G) \left(\frac{z}{\rho} \right)' \\ F_3 &= -(1 + G\gamma) + (1 + G\gamma)\rho x''. \end{aligned} \quad (5)$$

Here, θ is the orbital angle that remains constant outside the bends. Although the spinor function Ψ is similar in form to the quantum-mechanical-state function, in this case \vec{S} is a classical vector. However, as in the former case, this two-component spinor is defined,

$$\Psi = \begin{pmatrix} u \\ d \end{pmatrix}. \quad (6)$$

u and d are complex numbers representing the up- and down-components. The components of the spin vector become

$$\begin{aligned} S_1 &= u^*d + ud^* \\ S_2 &= -i(u^*d - ud^*) \\ S_3 &= |u|^2 - |d|^2. \end{aligned} \quad (7)$$

Because $H = (\vec{\sigma} \cdot \vec{n})$ is hermitian,

$$|\vec{S}| = |u|^2 + |d|^2 = \Psi^\dagger \Psi \quad (8)$$

and the magnitude of the spin-vector remains constant. We chose the normalization condition for the spinor function to be $\Psi^\dagger\Psi = 1$. Moving to the Interaction frame using the transformation:

$$\begin{aligned}\Psi(\theta) &= \exp\left(-\frac{i}{2}\int_0^\theta f_3(t)dt\hat{\sigma}_z\right)\Psi_I(\theta) \\ \hat{\xi}(\theta) &= \xi(\theta)\exp\left(i\int_0^\theta f_3(t)dt\right),\end{aligned}\quad (9)$$

yields the following:

$$\begin{aligned}\frac{d\Psi_I^+}{d\theta} &= \frac{i}{2}\hat{\xi}\Psi_I^- \\ \frac{d\Psi_I^-}{d\theta} &= \frac{i}{2}\hat{\xi}^*\Psi_I^+.\end{aligned}\quad (10)$$

These equations can be cast into a standard 2^{nd} order homogeneous linear differential equation with variable coefficients,

$$\frac{d^2\Psi_I^+}{d\theta^2} - \left(if_3(\theta) + \frac{\xi'(\theta)}{\xi(\theta)}\right)\frac{d\Psi_I^+}{d\theta} + \frac{\xi(\theta)\xi(\theta)^*}{4}\Psi_I^+ = 0.\quad (11)$$

When evaluating the cumulative effect of the lattice on the spin, the standard approach is to expand $F_1 - iF_2$ into a multiperiodic series:

$$\xi(\theta) = F_1 - iF_2 = \sum_K \varepsilon_K e^{-iK\theta}.\quad (12)$$

Upon analyzing $\hat{\xi}$ one finds the frequencies are of the form $K = M + \ell_z\nu_z + \ell_x\nu_x$, where M is an integer, $\ell_{x,z} = -1, 0, 1$ and $\nu_{z,x}$ are the vertical and horizontal tunes. The resonance strength ε_K is:

$$\varepsilon_K = -\frac{1}{2\pi} \oint \left[(1 + G\gamma)(\rho z'' + iz') - i\rho(1 + G)\left(\frac{z}{\rho}\right)' \right] e^{iK\theta} d\theta.\quad (13)$$

Also usually the $(1 + G\gamma)\rho x''$ term is ignored to first order, so $\ell_x = 0$. Since θ is constant in a region without dipoles, it is usually clearer to express the resonance integral in terms of s :

$$\varepsilon_K = -\frac{1}{2\pi} \oint \left[(1 + G\gamma)\left(z'' + \frac{iz'}{\rho}\right) - i(1 + G)\left(\frac{z}{\rho}\right)' \right] e^{iK\theta(s)} ds.\quad (14)$$

For well isolated resonances the amount of depolarization caused by acceleration through any given spin resonance can be evaluated using the Froissart-Stora formula²

$$\frac{P_f}{P_i} = 2e^{-(\pi|\varepsilon_K|^2/2\alpha)} - 1,\quad (15)$$

where,

$$\alpha = \frac{1}{\omega_{rev}} \frac{d\nu_s}{dt}\quad (16)$$

is the spin tune crossing rate divided by the angular revolution frequency ω_{rev} , and $\frac{P_f}{P_i}$ is the ratio of initial vertical to final vertical polarization. For a flat orbit in a constant vertical field $\alpha \approx d(G\gamma)/d\theta$. The Froissart-Stora formula represents a solution to the T-BMT equation for the special case of crossing an isolated spin resonance.

Evaluation of Eq. (14) shows that there are several classes of spin resonances. They all can be related back to the vertical motion of the beam through the quadrupoles. This is because quadrupoles are the primary places in the lattice where the particle experiences horizontal magnetic fields which are capable of perturbing the spin from its vertical orientation. Thus its useful to decompose the vertical beam motion into its betatron part (z_β) and closed orbit piece (z_{co}).

$$z = z_\beta + z_{co}\quad (17)$$

Thus the spin resonances can be attributed these two terms. The first type are called intrinsic, which are due to the natural betatron motion. Their strength is proportional to the action of the particle and they live whenever $G\gamma = K = N \pm Q_z$. Here N is an arbitrary integer and Q_z is the vertical betatron tune. The second class is called imperfection spin resonances and are due to the vertical closed orbit distortions. They occur at $G\gamma = K = N$.

There are also of course other spin resonances for example due to linear betatron coupling and synchrotron sideband. However these are usually much weaker than these first two class of resonance.

III. RESONANCE FREE DESIGN

If one evaluates the contributions to the integral in Eq. (14) we see that integrand is function of z'' , z' and $(\frac{z}{\rho})'$. All of these factors are proportional to the strength and periodicity of the quadrupoles. In the case of a perfectly circular ring, (no straight sections), they can only contribute when K is equal to $Pn \pm Q_z$ where P is the periodicity of the lattice and n and arbitrary integer. This is essentially what has been shown in S.Y. Lee's book¹ in his calculation of the so-called enhancement functions which appear in the evaluation of Eq. (14),

$$\begin{aligned}\zeta_P\left(\frac{K \pm Q_z}{P}\right) \\ \zeta_P(x) = \frac{\sin(P\pi x)}{\sin(\pi x)}.\end{aligned}\quad (18)$$

Thus if we design a true ring lattice with super-periodicity equal to $P=48$ and a vertical tune with the integer part near 48 we should be able to accelerate up to $G\gamma = 48$ with out crossing any significant intrinsic resonances. This is because the electron energy range

from 100 MeV to 20 GeV corresponds to $0.24 < G\gamma < 45.5$. Thus the relevant spin resonances will occur at $0.23 < |K| < 45.5$. The first two important spin resonances associated with this type of lattice will occur at $K = P - 48.\nu_z = \nu_z$ and $K = 2P - 48.\nu_z = 48.\nu_z$ (here ν_z is the fractional part of the tune).

However we really want the ring to fit into the existing RHIC tunnel so we are stuck with the natural super-periodicity of six. If we consider that the spin precession which advances $G\gamma$, occurs in the dipoles, one can recover the 48 super-periodicity from the point of view of $G\gamma$ precession. This can be accomplished, if we are careful in how we construct the straight sections and make them so that the integral of Eq. (14) goes to zero. In this way if we maintain the super-periodicity of 48 in the arcs we should maintain the same intrinsic resonance structure of the pure ring (see Fig. 2). A side benefit is that in addition

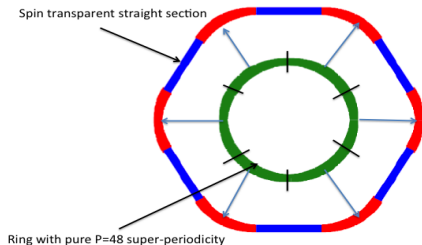


FIG. 2. Projecting the pure ring lattice with 48 super-periodicity onto the RHIC six fold periodic ring. If we keep the straight sections spin transparent then we can maintain the 48 super-periodicity.

to the intrinsic resonances, the imperfection resonances should also be minimized due to the design of this lattice. This is because the strongest imperfection resonances, like the intrinsic resonances for a pure ring, will be at $nP \pm [Q_z]$ where $[Q_z]$ indicates the integer part of the tune.

IV. PERFORMANCE

Following the principles outlined in the previous section we have constructed a lattice to fit into the existing RHIC tunnel. We first consider the performance of an ideal error free lattice. The DEPOL calculated intrinsic resonance structure follow, as was predicted, with negligible strength until $G\gamma$ reaches 48 (see Fig. 3). Tracking with this error free lattice also demonstrated no source of polarization loss out to emittances in excess of 1000 mm-mrad normalized. One reaches the end of the dynamic aperture before depolarization is possible. For these and future tracking we considered ramp rates which corresponded to 5 msec or 400 turns to 20 GeV. We also con-

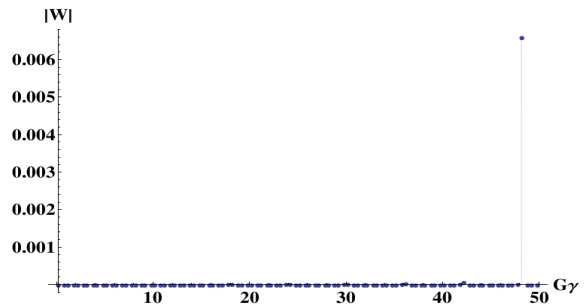


FIG. 3. Intrinsic Resonance Strength'

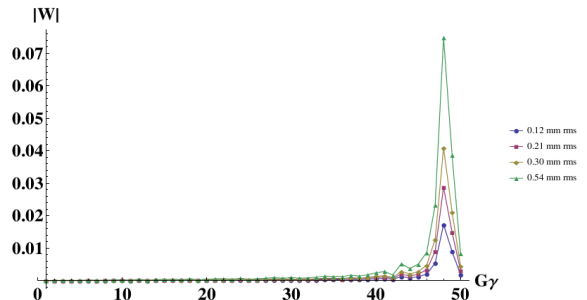


FIG. 4. Imperfection Resonance Strength'

sidered 10 times this amount or 50 msec or 4000 turns to 20 GeV to understand the limits and effect of ramp rate on polarization losses.

We also wanted to understand the field tolerances for this idealize lattice structure. We found that the addition of up to 0.1% in field errors had no significant impact on the calculated intrinsic resonances. This was also born out by tracking results.

Next we considered the effect of closed orbit errors and the associated imperfection resonance which they cause. In Fig. 4 the DEPOL calculated imperfection resonances are shown for different closed orbit errors. Again we can see the behavior is as predicted, with the first strong imperfection occurring at $G\gamma = 48$ below our 45.5 extraction $G\gamma$. Still in this case imperfection resonances below 45.5 are not insignificant and could constitute an important source of polarization loss.

A. Zgoubi Tracking Results

In Fig. 5 we see results from tracking with Zgoubi³ for the same closed orbit errors in Fig. 4. We see that even at 10 times slower rate than what is anticipated for this accelerator we can tolerate closed orbit errors less than 0.12 mm rms for $G\gamma$ values greater than 44. Below this we should be able to tolerate as high as 0.3 mm rms. In Fig. 6 we show the tracking results for the 0.3 mm rms case, now comparing it to the nominal acceleration rate of 5 msec. For the existing RHIC operations we typically see rms orbit errors on the level of 0.1 mm at

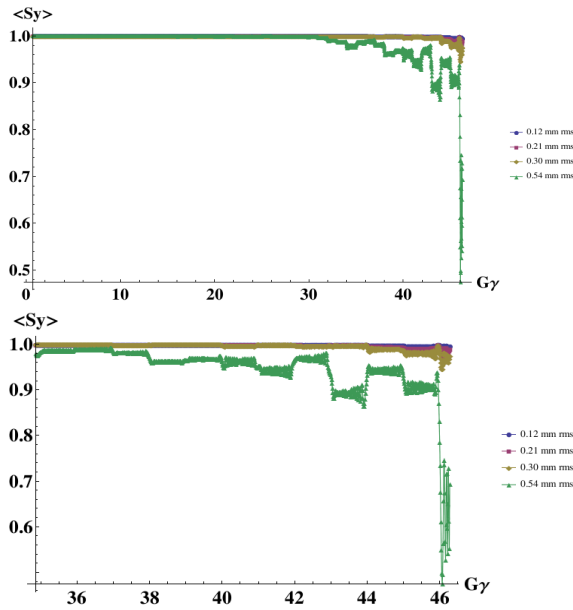


FIG. 5. Zgoubi 8 particle tracking using 50 msec ramp rate with 0.54, 0.3, 0.21 and 0.12 mm rms closed orbit errors. Plot of $G\gamma = 0$ to 46 (top) with a zoom from $G\gamma = 0$ to 46 (bottom).

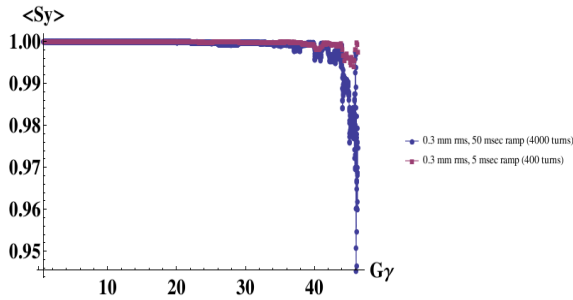


FIG. 6. Effect of ramp rate 5 versus 50 msec ramp rate with closed orbit errors of 0.3 mm rms.

injection and 0.04 mm at store.

In addition to closed orbit we wanted to understand the impact that rolls in the magnets could have on our polarization. Since DEPOL cannot correctly calculate non-planar spin resonances we had to rely on spin tracking. Quadrupole rolls should impact the betatron coupling present in the lattice. This in turn generates a coupled intrinsic spin resonance. However since the magnitude of the coupled intrinsic spin resonance is both proportional to and less than the normal intrinsic resonance we didn't anticipate any significant effects due to quadrupole rolls. This is actually what was observed. We saw no appreciable effect with rolls as high as 0.1 rad rms.

Rolls to the dipole however did effect the polarization to an appreciable extent. Observation of the spin tracking results shown in Fig. 7 - 9 show that we can only tolerate a dipole rolls less than 0.5 mrad rms. Also we can see that the impact seems to be on the imperfection

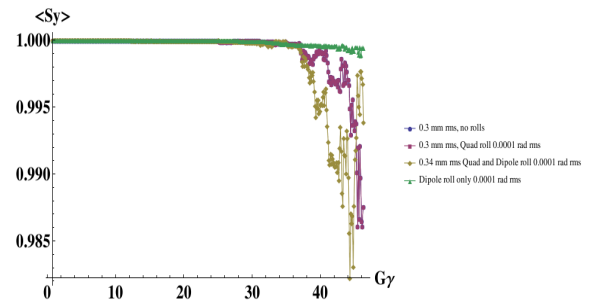


FIG. 7. Zgoubi 8 particle tracking using 5 msec ramp rate.

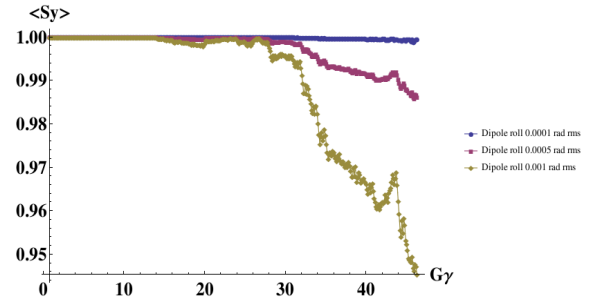


FIG. 8. Zgoubi 8 particle tracking using 5 msec ramp rate with only Dipole Rolls.

resonances primarily since when we accelerate at a slower rate we can see the depolarization occurring when $G\gamma =$ integer.

V. ACHIEVABLE RAMP RATE

Can we build a cost and risk effective system to take us from 200 MeV to 20 GeV in under 50 msec? From the point of view of ramping the magnetic field of the dipoles, this should be achievable. The dipoles for this lattice have a length of 4.64 meters with a bend angle of 0.016363 rad at 20 GeV they will reach a peak field of 0.22 Tesla in 50 msec (20 Hz) or achieve a rate of 4.4 T/sec, at 5 msec this is 44 T/sec. As a comparison the ISIS ring at Rutherford Lab reaches 0.7 Tesla at 50 Hz

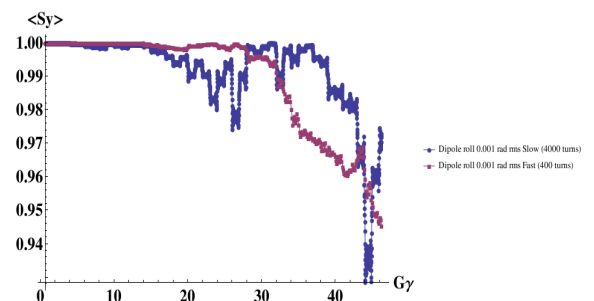


FIG. 9. Effect of ramp rate 5 versus 50 msec ramp rate.

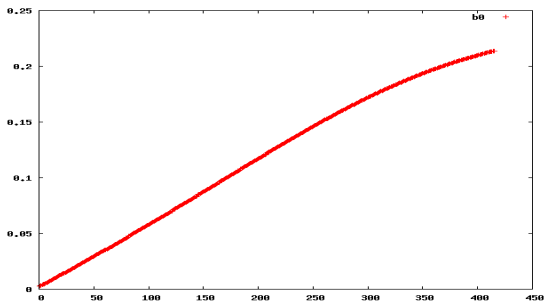


FIG. 10. Dipole field strength in Tesla versus turn number for an 60 MV per turn fixed phase acceleration. (5 msec ramp rate)

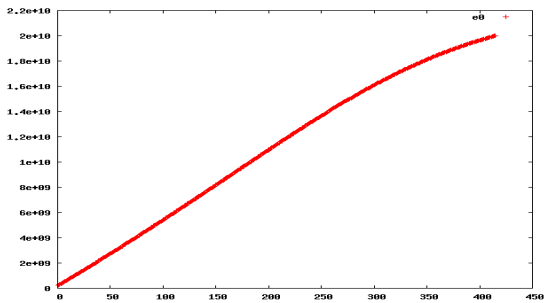


FIG. 11. Energy in eV versus turn number for an 60 MV per turn fixed phase acceleration. (5 msec ramp rate)

which translates into 35 T/sec.

From the point of view of the rf system, this might be more challenging. If we account for radiation power loss we can get to top energy over approximately 400 turns using a single cavity powered at a fixed 60 MV per turn and fixed phase. In Fig. 10 we can see the calculated dipole field trajectory as a function of turn number and in Fig. 11 the calculated energy as a function of turn

number for this system. The outstanding question is the risk and cost associated with the construction of such an rf system.

VI. FEASIBILITY OF SLOWER RAMP RATE

If we reduce our ramp rate to 500 msec then the tolerances on the orbit might be very difficult to reach. However this might be solved by introducing a partial solenoidal snake somewhat similar to what we use to have in the AGS (5-10% snake). This could be achieved using 7.24 m solenoid ramped from 0.02 T to 4 T over half a second during acceleration from 200 MeV to 20 GeV. This will take care of the imperfections, however care must be taken so that it doesn't break the symmetry too much and introduce intrinsic resonances that are too large. We are currently studying this option.

VII. CONCLUSION

The effect of intrinsic resonances for this proposed lattice are non-existent (we will run out of aperture before they can effect the spin). The major effect comes from imperfections and dipole rolls. It can handle up 0.3 mm rms orbit distortion for the 50 msec ramp. This is what RHIC easily does currently. Also these orbit tolerance are in force only at the top end of the ramp, at $G\gamma$ above 44. Below 30 $G\gamma$ we could tolerate much more than 0.54 mm rms. We can handle effects due to dipole rolls less than 0.5 mrad rms.

The proposed ramp rate is achievable from the point of view of the dipole field, however the performance of the RF system is still an outstanding question. It's performance would be a function of the total current and the achievable peak accelerating fields and achievable cycle rate, constrained by mechanical stress. If necessary slower ramp rates might be feasible with the introduction of a ramp solenoid partial snake. This is currently under study.

¹ S. Y. Lee, *Spin Dynamics and Snakes in Synchrotrons* (World Scientific Pub Co Inc, 1997).

² M. Froissart and R. Stora, Nucl. Inst. Meth. **7**, 297 (1960).

³ F. Meot, "Zgoubi," <https://sourceforge.net/projects/zgoubi/files/> (2015).